(2)

FIRST ANNUAL TECHNICAL REPORT

on

ONR Grant No.: N00014-90-J-4039

(July 1, 1990 to June 30, 1991)

by

Dr. Chen S. Tsai

Professor and Principal Investigator

Department of Electrical and Computer Engineering

and

Institute for Surface and Interface Science

University of California, Irvine

Irvine, California 92717

Magnetostatic Waves-Based Integrated Optic Bragg Cell Modules With Applications To RF Signal Processing

(ONR Grant No.: N00014-90-J-4039)

First Annual Technical Report

Dr. Chen S. Tsai

Principal Investigator

SUMMARY OF PROGRESS

Two major achievements have been made during the first program year (July 1, 1990 to June 30, 1991): First, a compact magnetostatic forward volume wave-based guided-wave magnetooptic (MO) Bragg cell module has been realized by utilizing a small permanent magnet together with a current-carrying tuning coil. Performance characteristics comparable to those obtained using the bulky electromagnet have been obtained. Second, magnetostatic backward volume wave-based guided-wave MO Bragg cells have been realized, for the first time, and used to perform wide-angle light beam scanning by tuning the carrier frequency from UHF- to X-band.

I. INTRODUCTION AND OBJECTIVE

Although Magneto-optics in waveguide structures [1] was among the areas actively pursued during the early phase of Guided-Wave Optics research, research activity in this area was greatly reduced between the mid 70's and early 80's. However, a revival of interest in this area has taken place recently. One subject of this renewed interest concerns collinear [2] and noncollinear (transverse Bragg) [3] magnetooptic (MO) interactions between guided-optical waves (GOW) and magnetostatic waves (MSW) in Yittrium Iron Garnet-Gadolinium Gallium Garnet (YIG-GGG) waveguides. MSWs are slow-propagating electromagnetic waves which result from propagation of electron spin

precession around a DC magnetic field in a thin film of ferromagnetic material such as YIG on a suitable substrate such as GGG. MSWs have their energy confined in a small depth beneath the ferromagnetic film, and can be readily and efficiently generated by applying a microwave signal to a short-circuited metallic strip brought into close proximity. The center frequency of the MSWs can be tuned, typically from 1.0 to higher than 20 GHz simply by varying the DC magnetic field. Guided-wave MO interactions result from the moving optical grating induced by the MSW through the Faraday and Cotton-Mouton effects, similar to a guided-wave acoustooptic (AO) interaction [4] in which the surface acoustic wave (SAW) induces a moving optical grating through the photoelastic effect. The periodicity of the resulting optical grating is determined by the dispersive relation between the velocity and the frequency of the MSW as a function of the DC magnetic field. In a noncollinear [3] coplanar geometry as shown in Fig. 1, a portion of an incident light is Bragg diffracted and mode-converted as a result. The resulting MO Bragg modulators are called MO Bragg cells [5] in analogy with the prevalent AO Bragg cells.

In comparison to their AO counterparts, the unique advantages associated with the MO Bragg cells are: 1. A much larger range of tunable carrier frequencies may be obtained by varying the DC magnetic field [6]. Such high and tunable carrier frequencies with the MO devices allows direct processing at the carrier frequency of wideband RF signals and eliminated the need for indirect processing via frequency down-conversion as is required with the AO devices; 2. A large MO bandwidth may be realized by means of a simpler transducer [5]; and 3. Much higher and electronically tunable modulation/switching and scanning speeds are achievable as the velocity of propagation for the MSWs can be higher than that of the SAWs by one- to two-orders of magnitude [7].

The objective of this ONR-sponsored research is to explore the potential of the magnetostatic waves-based integrated MO Bragg cell modules for applications in real-time processing of wideband RF signals at microwave carrier frequencies.

REFERENCES

[1] See, for example, P.K. Tien, R.J. Martin, R. Wolfe, R.C. LeCraw and S.L. Bank, "Switching and Modulation of Light in Magneto-Optic Waveguides of Garnet Films," Appl. Phys. Lett., Vol. 21, pp. 394-396 (1972).

[2] A.D. Fisher, J.N. Lee, E.S. Gaynor, and A.B. Tveten, "Optical Guided-Wave Interactions with Magnetostatic Waves at Microwave Frequencies," Appl. Phys. Lett, vol. 41, pp. 779-781 (Nov. 1982).

[3] (a) C.S. Tsai, "Hybrid Integrated Optic Modules for Real-Time Signal Processing," Proc. of NASA Optical Information Processing Conference II, NASA Conference Publication No. 2302, pp. 149-164 (1983);

(b) C.S. Tsai, D. Young, W. Chen, L. Adkins, C.C. Lee and H. Glass, "Noncollinear Coplanar Magneto-Optic Interaction of Guided Optical Wave and Magnetostatic Surface Waves in Yttrium Iron Garnet-Gadolinium Gallium Garnet Waveguides," Appl. Phys. Lett., vol. 47, pp. 651-654 (Oct. 1985).

[4] C.S. Tsai, "Guided-wave Acoustooptic Bragg Modulators for Wide-Band Integrated Optic Communications and Signal Processing," IEEE Trans. on Circuits and System, vol. CAS-26, pp. 1072-1098 (Dec. 1979).

[5] D.Young and C.S. Tsai, "GHz Bandwidth Magnetooptic Interaction in YIG-GGG Waveguide Using Magnetostatic Forward Volume Waves," Appl. Phys. Lett., vol. 53, pp. 1696-1698 (Oct. 1988).

[6] D. Young and C.S. Tsai, "X-Band Magnetooptic Bragg Cells using Bismuth-Doped Yttrium Iron Garnet Waveguides," Appl. Phys. Lett., vol. 55, pp. 2242-2244 (Nov. 1989).

[7] C.S. Tsai and D. Young, "Wideband Scanning of Guided-Light Beam and RF Spectral Analysis Using Magnetostatic Forward Volume Waves in YIG-GGG Waveguide," Appl. Phys. Lett., vol. 54, pp. 196-198 (Jan. 1989).

II. MAJOR PROGRESS

During the first program year two major advances were made: 1. Miniaturization, for the first time, of the MO Bragg cell that utilizes magnetostatic forward volume wave (MSFVW), and 2. Realization, for the first time, of MO Bragg cells that utilize magnetostatic backward volume wave (MSBVW). A detail report on each now follows.

1. Compact Magnetostatic Forward Volume Wave-Based Magnetooptic Bragg Cell Module by Utilizing Small Permanent Magnet

Abstract

Compact magnetostatic forward volume wave-based guided-wave magnetooptic (MO) Bragg cell modules have been realized by utilizing a pair of small samarium-cobalt permanent magnets together with a pair of current-carrying coils. Highly uniform DC magnetic field in the air gap where yttrium iron garnet-gadolinium gallium garnet (YIG-GGG) waveguide samples are inserted has been obtained. Tunable DC magnetic field as large as 2446 Oe corresponding to a tunable carrier frequency band of 6.85 GHz has been achieved. The resulting MO Bragg cell modules with carrier frequencies ranging from 2.0 to 12.0 GHz have provided performance characteristics comparable to those obtained by using a bulk electromagnet at the optical wavelength of 1.303 μm. Compact MO Bragg cell modules of even higher carrier frequency, higher range of tunable carrier frequency and smaller sizes can be constructed to facilitate their potential applications such as modulation, scanning and switching of light beam as well as real-time processing of wideband microwave signals without requiring frequency down-conversion.

Detailed Description of Progress

A new class of optical devices called the guided-wave magnetooptic (MO) Bragg cells [1] that are potentially capable of providing desirable features similar to that of the now prevalent acoustooptic (AO) Bragg cells, but potentially at superior performance characteristics have been reported recently [2,3]. For example, wideband MO Bragg cells

using pure yttrium iron garnet-gadolinium gallium garnet (YIG-GGG) and Bi-doped YIG-GGG waveguide samples have been fabricated and operated at tunable carrier frequencies ranging from 2 to 12 GHz [2,3]. Such guided-wave MO Bragg cells possess the unique advantages of very high and tunable carrier frequencies, tunable dispersion relation, large bandwidth, and compatibility with monolithic microwave integrated circuits (MMIC) and hybrid integrated circuits (HIC) technologies. However, all the works on guided-wave MO interactions and related devices reported heretofore (see the many references cited in Ref. 1) had employed bulky electromagnets to provide the DC magnetic fields for excitation of the types of magnetostatic waves involved. The obvious disadvantages associated with such electromagnets include the very large weight and size, the requirement for a bulky cooling system, the lack of robustness, and the high cost. In this paper, we report the first realization of compact guided-wave MO Bragg cell modules using a pair of small permanent magnets together with a pair of current-carrying coils.

Fig. 1 shows the sketch of the compact magnetostatic forward volume wave (MSFVW)-based MO Bragg cell module to be reported. The pair of permanent magnets, each 1" x 1" x 0.25" in size, are made of samarium-cobalt (Sm-Co) which has the magnetic energy product of 16 x 10^6 Gauss-Oe. The pole pieces of smaller cross sectional area were used to concentrate the magnetic flux and provide a more uniform magnetic field in the air gap where the YIG-GGG waveguide sample is to be inserted. The current-carrying coils were wound on the nylon robins and placed around the pole pieces in order to facilitate variation of the magnetic field in the air gap.

The resulting magnetic circuit may be analyzed in the manner similar to electric circuits. Since the magnetic field generated by the permanent magnets will not be affected by the external magnetomotive force, we will consider only the field generated by the coils, which will be consumed in the air gap and inside the steel segment. The external magnetomotive force NI require is determined by the following equation [4]:

$$NI = H_g l_g + \Sigma H_s l_s \qquad (1)$$

where $H_g l_g$ and $\Sigma H_s l_s$ represent, respectively, the magnetomotive forces required to establish a magnetic field intensity of H_g across an air gap of l_g, and H_s in the steel segment of length l_s in the circuit. Here N is the number of turns in the coil, and I is the DC current in the coil in ampere. Although the NI required can not be determined exactly due to insufficient informations about the steel segment, it can be shown [5] that an amount varying between 10 to 25 percent of the magnetomotive force required for the air gap will be consumed in the steel segment; and that additional 5 to 10 percent of the air gap magnetomotive force is needed to account for the discontinuity between the steel segments. Thus Eq. (1) may be solved empirically for the NI by substituting $\Sigma H_s l_s$ with (0.15 to 0.35) x $H_g l_g$. Therefore, we have

$$NI = (1.15 \text{ to } 1.35) \times H_g l_g \qquad (2)$$

For example, at H_g = 750 Oe and l_g = 5.0 mm the required NI is equal to 1.35 x 750 x (5/25/4) x 2.02 amp-turn = 400 amp-turn. Note that a factor of 1.35 and a conversion factor of 1 Oe = 2.02 amp-turn per inch are used in this calculation.

As depicted in Fig. 1, the DC magnetic field intensity in the air gap, H_0, can be tuned by using either of three methods, namely, variation of the gap between the magnet pair through a micrometer, variation of the current through the coils, and variations of both the gap and the current. The magnet wire used for the coils has the size of 28 a.w.g. and the number of turns in each coil is around 520. The measured magnetic field intensity as a function of the gap varied through the micrometer at the absence of current is shown in Fig.2(a). It is seen that the DC magnetic field intensity can be varied from 1600 to 4126 Oe. The figure shows that higher magnetic field intensity can be obtained by reducing the air gap further. Thus based on the well-known ferromagnetic resonance relation $\omega_0 = \gamma H_i$ in which ω_0 corresponds to the center frequency of the resulting magnetostatic wave, γ the gyromagnetic ratio (2.8 MHz/Oe), and H_i the internal magnetic field ($=H_0 - 4\pi M_s + H_a$, where $4\pi M_s$ = 1750 Oe and 1800 Oe for pure YIG and Bi-YIG samples, respectively, is the saturation magnetization and H_a = 150 Oe and 1660 Oe, is the corresponding

anisotropic field [1]) in the YIG-GGG sample, the center frequency of the resulting MO Bragg cells may be tuned over the range of 2.0 to 12.0 GHz. Since an even higher magnetic field can be obtained [6] by using a NdFeB permanent magnet which carries a higher magnetic energy product of 28 x 10^6 Gauss-Oe, it should be possible to extend the center frequency up to 20.0 GHz. It should be noted that a motor-driven activator may be used to provide a much finer and faster mechanical tuning, and thus fast and fine tuning of the center frequency.

Fig.2(b) shows the measured changes in the magnetic field intensity (ΔH_0) induced by a current of 0.85 Amp as a function of the air gap. It is seen that maximum change as high as 2446 Oe was measured at the air gap of 6.16mm. This current-controlled changes in DC magnetic field intensity correspond to a carrier frequency tuning bandwidth as high as 6.85 GHz. Note that in Eq. (2) we have estimated a factor of 1.15 to 1.35 be used to account for the magnetic losses in the circuit. However, the data of Fig.2(b) suggests that a factor of 1.46 should be used instead by plugging the values of H_g and l_g into Eq. (2). The higher loss could be due to the material used for the magnetic circuit and the leakages through fringing effect. For a cross sectional area identical to an effective device sample size of 5 x 5 mm^2, i.e., the MSFVWs generated from a transducer aperture of 5.0 mm and a propagation path of 5.0 mm in the YIG-GGG sample, the uniformity of the magnetic field intensity was measured to be within 0.05% when the air gap was set at 6.16 mm, and 1.9% when the air gap was increased to 10.16 mm.

Both pure and Bi-doped YIG-GGG waveguide samples having, respectively, 4.2 and 3.5 μm YIG layer thickness were used in the construction of the compact MSFVW-based MO Bragg cells with their carrier frequencies tuned from 2.0 to 12.0 GHz. Measurements of performance characteristics were carried out at the optical wavelength of 1.303 μm using the setup and procedure described in Ref.[1]. Fig.3(a) shows that a -3dB MO bandwidth of 250 MHz was measured at the center frequency of 3860 MHz and H_0 of 2900 Oe for the pure YIG Bragg cell. In the present experiment, the thickness of the pure YIG waveguide

is 4.2 μm and the transducer width is 60 μm. The calculated bandwidth [7] for the device parameters and magnetic field involved is 255 MHz. For the Bi-doped YIG Bragg cell, a -3dB MO bandwidth of 200 MHz measured at 7600 MHz and H_0 of 2805 Oe as shown in Fig. 3(b), as opposed to a calculated bandwidth of 230 MHz, was found to be comparable to that measured with the Bragg cell using a bulk electromagnet[1]. Finally, a 26 dB linear dynamic range was measured at the carrier frequency of 3860 MHz for the pure YIG Bragg cell. Compared to the 12 dB linear dynamic range measured previously, the increase of 14 dB is due to larger output power of the laser diode used. Fig. 4 shows the measured relative diffraction efficiency versus the RF drive power at the carrier frequency of 7600 MHz for the Bi-doped YIG Bragg cell. Clearly, the same dynamic range of 40 dB[3] has been reproduced. In the plot, the reference level (relative diffraction efficiency = 0 dB) corresponds to a diffraction efficiency of 7.14% measured at an RF drive power of 28.2 dBm (660 mW) (or a corresponding calculated MSFVW power of 20 mW). This measured diffraction efficiency is comparable to that measured using the bulky electromagnet. For RF drive powers higher than 28.2 dBm, some deviation from linearity between the diffraction efficiency and the RF drive power was observed.

Two types of light beam scanning experiments were carried out: one with the frequency of the MSFVW tuned continuously from the center frequency while keeping the DC magnetic field fixed, and the other with the DC magnetic field tuned continuously while keeping the frequency of the MSFVW fixed. Fig. 5(a) shows the photographs of scanned beam spots of a laser light at the wavelength of 1.303 μm using the Bi-doped YIG Bragg cell by varying the carrier frequency from 7640 to 7740 MHz at a fixed DC magnetic field of 2805 Oe. Fig.5(b) shows the photographs of scanned light beams by tuning the current from 0.0 to 0.07 amps that resulted in the variation of the DC magnetic field by 0 to 98 Oe from 2805 Oe. Also shown in Fig. 5(c) is the light beam scanning produced by the pure YIG Bragg cell. Finally, the measured dispersion relationship between the carrier

frequency and the wavenumber (propagation constant) relevant to the MO interaction was shown to be in good agreement with the calculated results [7].

In summary, compact MSFVW-based guided-wave magnetooptic MO Bragg cell modules with tunable carrier frequencies ranging from 2.0 to 12.0 GHz have been realized by utilizing a pair of small Sm-Co permanent magnets together with a pair of current-carrying coils. Performance characteristics comparable to those obtained using the bulky electromagnet have been reproduced. It is concluded that compact MO Bragg cell modules of even higher carrier frequency, higher range of tunable carrier frequency and smaller sizes can be constructed to facilitate their potential applications such as modulation, scanning [8] and switching of light beam as well as real-time processing of wideband microwave signals without requiring frequency down-conversion.

References

[1] C.S. Tsai and D. Young, "Magnetostatic-forward-volume-wave-based Guided-wave Magneto-optic Bragg Cells and Applications to Communications and Signal Processing," *IEEE Trans. on Microwave Theory and Techniques*, **38**, 560 (1990).

[2] D. Young and C.S. Tsai, "GHz bandwidth magnetooptic interaction in YIG-GGG waveguide using magnetostatic forward volume waves," *Appl. Phys. Lett.*, **53**, 1696 (1988).

[3] D. Young and C.S. Tsai, "X-band magnetooptic Bragg cells using bismuth-doped yttrium iron garnet waveguides," *Appl. Phys. Lett.*, **54**, 2242 (1989).

[4] R.L. Coren, **Basic Engineering Electromagnetics**, pp. 163-167, Prentice Hall, Englewood Cliffs, New Jersey, 1989.

[5] H.C. Roters, **Electromagnetic Devices**, pp. 246-249, John Wiley & Sons, Inc. New York, 1941.

[6] C.L. Wang, Y. Pu, and C.S. Tsai, "Compact Magnetostatic Wave-Based Magnetooptic Bragg Cell Module by Utilizing Small Permanent Magnet," To be presented

at 1991 Topical Meeting on Gradient-Index Optical Systems, April 8-9, Monterey, California.

[7] Y. Pu and C.S. Tsai, "Magnetization of Magnetostatic Forward Volume Wave in a YIG-GGG Layer Structure with Application to Guided-Wave Magnetooptic Bragg Cells," Proceeding of Ultrasonic Symposium, Honolulu, Dec. 1-7, 1990.

[8] C.S. Tsai and D. Young, "Wideband scanning of guided-light beam and RF spectral analysis using magnetostatic forward volume waves in YIG-GGG waveguides," *Appl. Phys. Lett.*, **54**, 196 (1989).

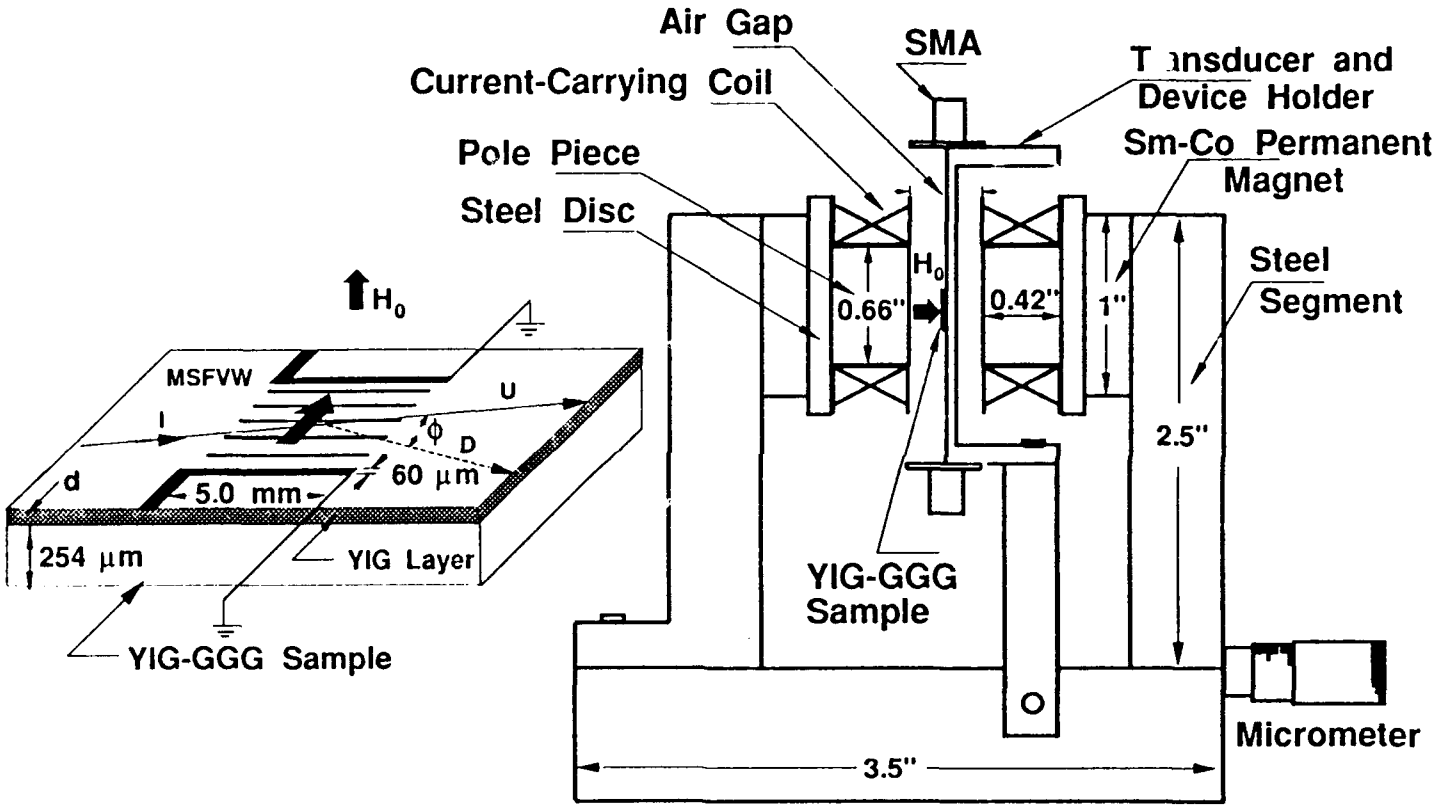

Fig. 1: Sketch Of Compact Magnetostatic Forward Volume Wave-Based MO Bragg Cell Module (In the inset: I: Incident Light, U: Undiffracted Light, D: Diffracted Light, d: Thickness of YIG)

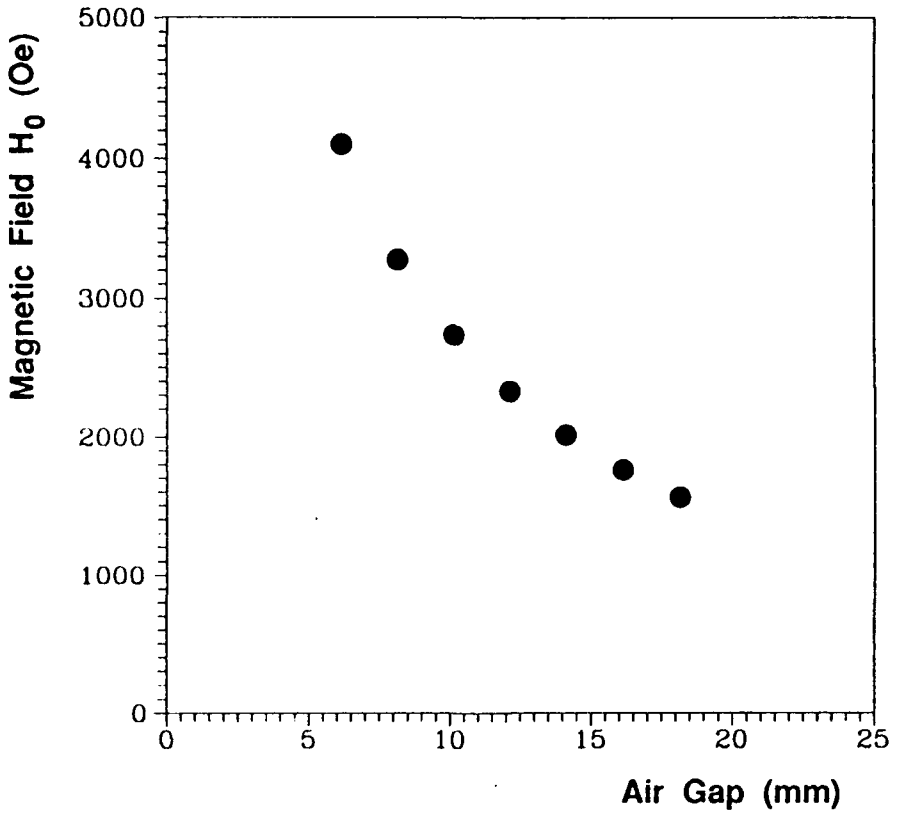

Fig. 2(a): DC Magnetic Field Versus The Air Gap Between A Pair Of Small Sm-Co Permanent Magnets

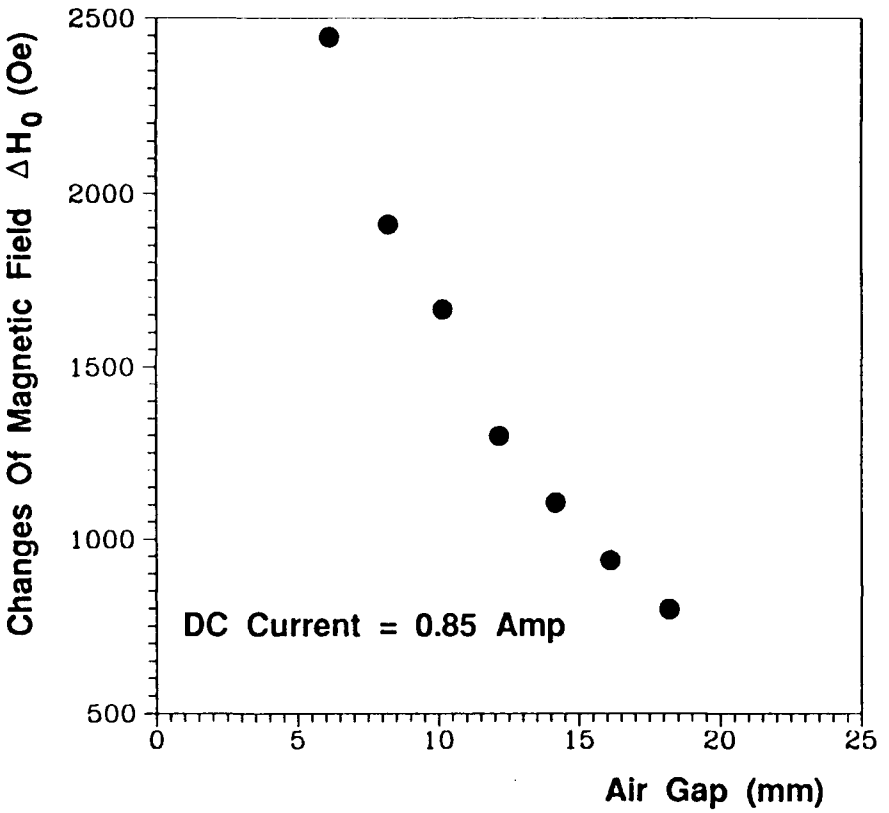

Fig. 2(b): Measured Changes Of Magnetic Field Induced By Current-Carrying Coils Versus The Air Gap

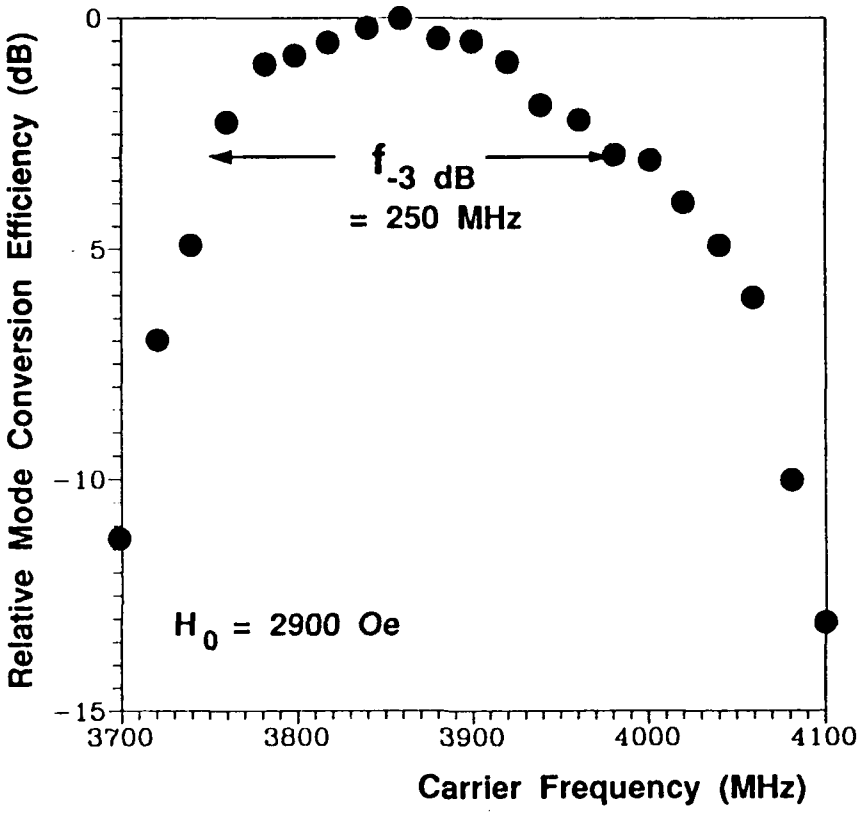

Fig. 3(a): Measured Relative Mode Conversion Efficiency Versus The Carrier Frequency Of MSFVW Centered At 3860 MHz For Pure YIG MO Bragg Cell

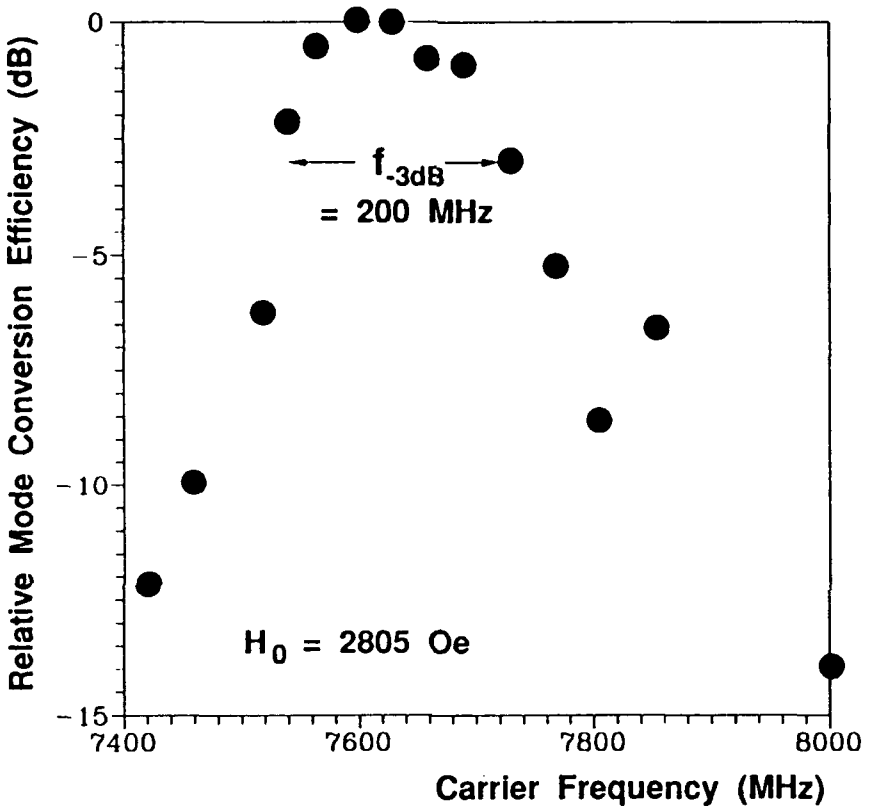

Fig. 3(b): Measured Relative Mode Conversion Efficiency Versus The Carrier Frequency Of MSFVW Centered At 7600 MHz For Bi-YIG MO Bragg Cell

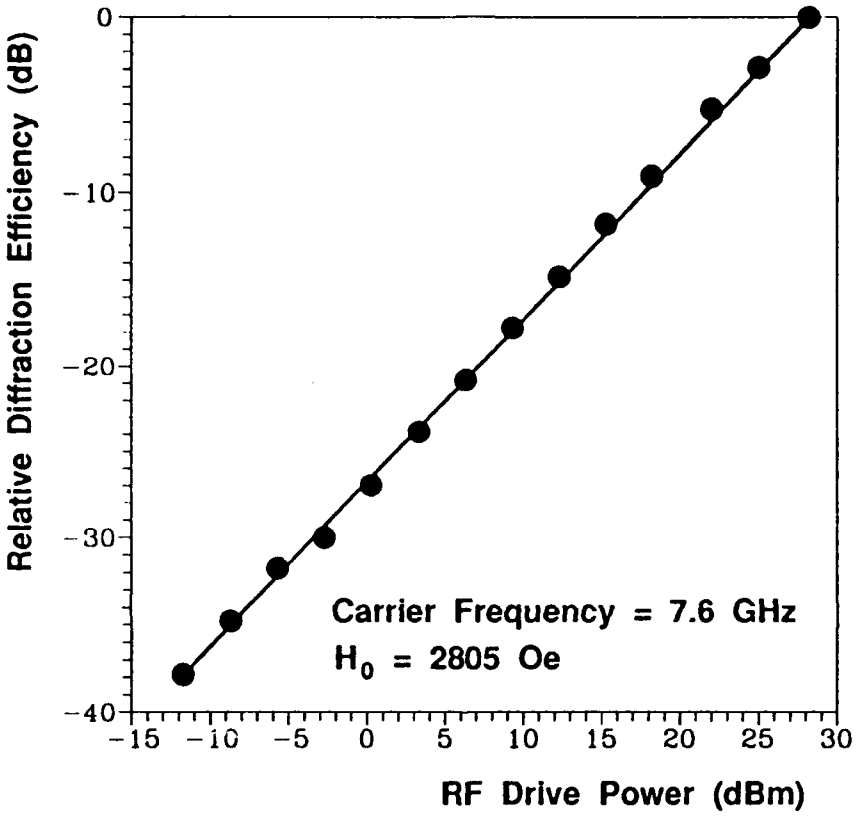

Fig.4: Relative Diffraction Efficiency Of Bi-doped YIG MO Bragg Cell Versus The RF Drvie Power

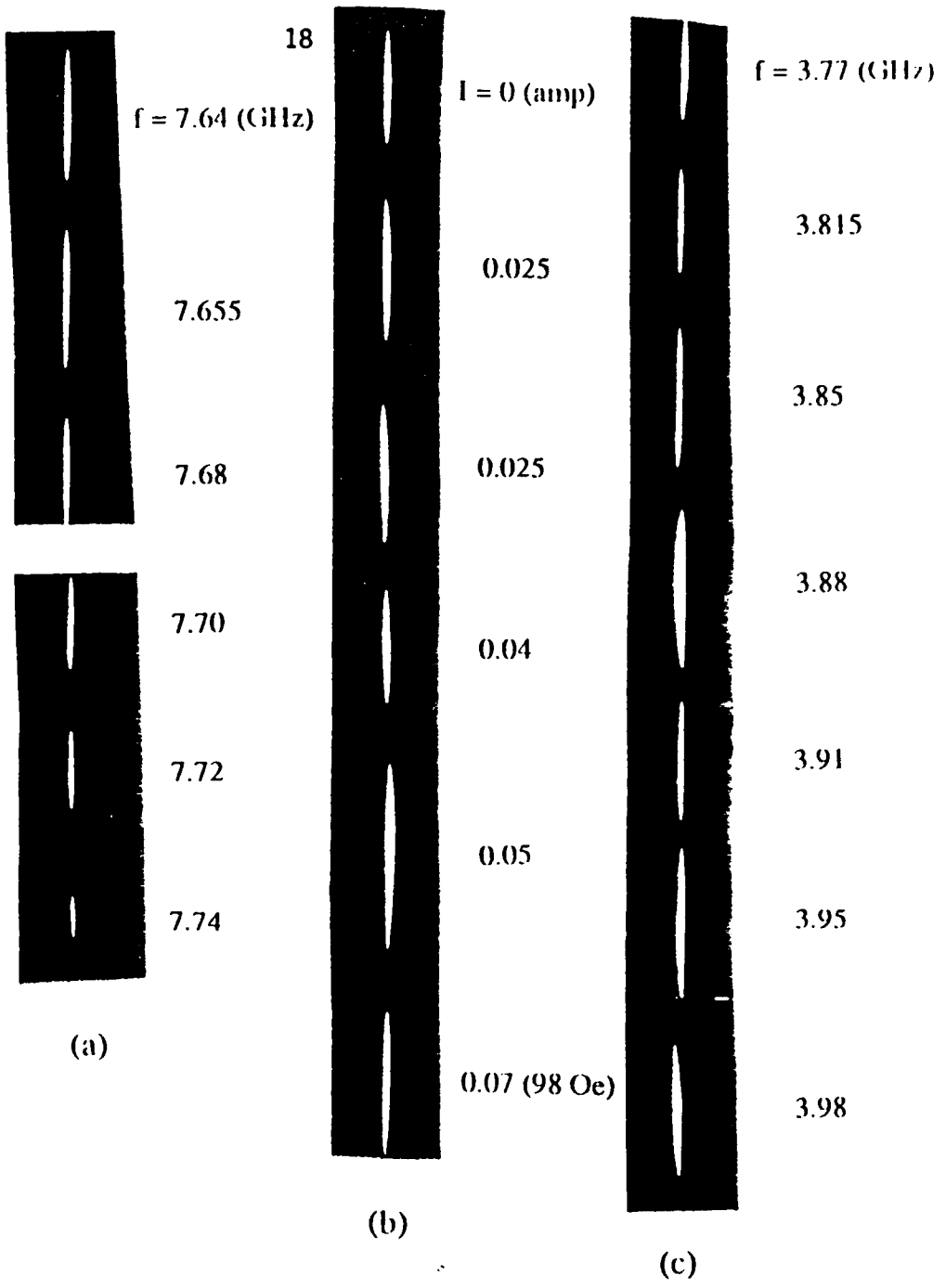

Fig. 5(a): Deflected Light Spots Obtained By Varying The Carrier Frequency Around 7680 MHz With The Bi-YIG MO Bragg Cell (H_0 = 2805 Oe)

(b): Deflected Light Spots Obtained By Varying The Current Through The Coils With The Bi-YIG MO Bragg Cell (Carrier Frequency = 7740 MHz)

(c): Deflected Light Spots Obtained By Varying The Carrier Frequency Around 3900 MHz With The Pure YIG MO Bragg Cell (H_0 = 2900 Oe)

2. Magnetostatic Backward Volume Wave-Based Magnetooptic Bragg Cells

Abstract

This paper reports the first realization of high-performance magnetostatic backward volume wave (MSBVW)-based magnetooptic (MO) Bragg cells in pure and bismuth-doped yttrium iron garnet-gadolinium gallium garnet (YIG-GGG) waveguides, and the first demonstration of wide-angle light beam scanning using such MO Bragg cells. The MSBVW-based MO Bragg cells have been shown to possess the following advantages over the magnetostatic forward volume wave (MSFVW)-based counterparts: (1) The center frequency of the former is higher by some 4.9 GHz at the same DC magnetic field, (2) The first passband in which the MO Bragg cells commonly operate is located at the high frequency end for the former, but at the low frequency end for the latter, and (3) The Bragg diffraction or mode-conversion efficiency of the MSBVW-based MO Bragg cells can be significantly higher than that of the MSFVW-based counterparts.

Detailed Description of Progress

Magnetostatic surface waves (MSSW) were utilized to realize the first guided-wave magnetooptic (MO) Bragg cell [1] in a pure yttrium iron garnet-gadolinium gallium garnet (YIG-GGG) waveguide [2]. Since both magnetostatic forward volume waves (MSFVW) and magnetostatic backward volume waves (MSBVW) carry a more uniform distribution of rf magnetizations along the normal direction of the optical waveguiding layer, a higher MO Bragg diffraction or mode-conversion efficiency is possible by using either of such volume waves. It is, therefore, desirable to realize guided-wave MO Bragg cells that utilize the MSFVW or the MSBVW. Wideband guided-wave MO Bragg diffraction by the MSFVW and the resulting MO Bragg cells were realized previously in pure YIG-GGG samples [3,4] and extended recently to Bismuth-doped YIG-GGG waveguide samples [5,6]. Guided-wave MO interaction with the MSBVW was first studied using a Bi Lu-YIG-GGG waveguide [7]. However, to the best of our knowledge, no study on guided-light beam scanning by the MSBVW has been reported heretofore. In this paper, we report the first

realization of high-performance MSBVW-based MO Bragg cells in pure and Bismuth-doped YIG-GGG waveguides, and the first demonstration of wide-angle light beam scanning using such MO Bragg cells.

The geometry and the dimensions of the MSBVW-based MO Bragg cells as well as the experimental arrangement are shown in Fig. 1. A homogeneous DC magnetic field H_o is applied in the waveguide plane and along the Y-axis to excite Y-propagating MSBVW using a microstrip line transducer. The rf magnetization of the MSBVW produces an optical grating through the dynamic Farady and Cotton-Mouton effects, which in turn results in coupling between the incident light in the TE_0-mode and the diffracted light in the TM_0-mode, and vice versa [1,8]. Analysis of the MO interaction involved has been carried out using the couple-mode technique[9]. Theoretically, the operating frequency bands of the MSBVW and the MSFVW, at a given H_o, are given by Eqs.(1) and (2), respectively [10]:

$$\text{MSBVW:}\quad \gamma(H_o+H_a) \text{ to } \gamma\sqrt{(H_o+H_a)(H_o+H_a+4\pi M_s)} \tag{1}$$

$$\text{MSFVW:}\quad \gamma(H_o+H_a-4\pi M_s) \text{ to } \gamma\sqrt{(H_o+H_a-4\pi M_s)(H_o+H_a)} \tag{2}$$

where γ designates the gyromagnetic ratio (2.8 MHz/Oe), $4\pi M_s$ the saturation magnetization, and H_a the magnetic anisotropy. From Eqs.(1) and (2), we see that the low frequency end of the MSBVW is higher than that of the MSFVW by about $\gamma 4\pi M_s$. Taking the pure-YIG sample as an example, we have $4\pi M_s$=1750 Oe and $4\pi M_s$=4.90 GHz. Fig.2(a) and (b) show the calculated MO Bragg diffraction or mode-conversion efficiency by, respectively, the MSBVW and the MSFVW under the assumptions of perfect phase-matching and ideal coupling of microwave in the transducer in a pure-YIG waveguide [11]. The dimensions of the transducers and the identical DC magnetic fields used in the calculation are shown in the insets. It is found that the first passband which incurs the lowest insertion loss and provides the largest -3dB bandwidth is located at the high frequency end for the MSBVW, but at the low frequency end for the MSFVW. This

finding shows that for the same DC magnetic field, the operating frequency band of the MSBVW-based MO Bragg cell is located higher than that of the MSFVW-based MO Bragg cell by at least 4.90 GHz for the pure YIG-GGG sample and 5.04 GHz for the Bi-YIG-GGG ($4\pi M_S$=1800 Oe) sample. From Fig. 2, it is also found that the peak diffraction efficiency achievable using the MSBVW is about 60% which is some 10% higher than that achievable using the MSFVW at the same DC magnetic field and microwave drive power. Our calculation also shows that the peak diffraction efficiency achievable using the MSBVW would be much higher than that achievable using the MSFVW at the same range of carrier frequency. For example, the peak diffraction efficiency achievable using the MSFVW would be only 12% when the center frequency of its first passband is shifted to coincide with that of the MSBVW shown in Fig.2(b).

In the experiment, an incident light wave at the wavelength of 1.303 μm was edge-coupled into the waveguide sample to excite a TE_0-mode guided-light propagating along the X axis. The measurement was performed using the techniques similar to those described in references [3] and [8]. The frequency responses of the resulting MSBVW-based MO Bragg cells at fixed DC magnetic fields were measured for both the pure YIG- and the Bi-YIG-GGG samples. Figs.3(a) and (b) present the data obtained at H_0=1000 and 2700 Oe for the pure YIG-GGG sample. The center frequencies were found to be 4.78 and 9.7 GHz, respectively. It is to be noted that for the MSFVW-based Bragg cells even the much lower center frequencies of 2.5 and 6.0 GHz (not shown) required DC magnetic fields as high as 2280 and 3500 Oe. Fig.3(c) shows the measured frequency response for the Bi-YIG-GGG sample at a center frequency of 6.1 GHz that required a DC magnetic field of only 1900 Oe. The -3dB MO bandwidth was measured to be 430 MHz which is a nearly three-fold increase over that obtained with the MSFVW-based Bragg cells [5] namely 150 MHz, at a DC magnetic field as high as 3637 Oe.

In our previous MSFVW experiment, the peak mode-conversion (diffraction) efficiencies were measured to be 0.54% at the carrier frequency of 6.0 GHz and the

MSFVW power (P_{MSFVW}) of 250mW in the pure YIG-GGG waveguide [3] and 12% at 7.35 GHz and 56mW in the Bi-YIG=GGG waveguide [5]. The corresponding microwave drive powers were 2000 and 2500mW. In the present MSBVW experiment, the peak efficiency measured is 1% at 4.78 GHz and the MSBVW power (P_{MSBVW}) of 153 mW in the pure YIG-GGG sample, and 15% at 6.22 gHz and 60mW in the Bi-YIG-GGG sample. The corresponding microwave drive powers are as low as 380 and 602 mW. The dc magnetic fields used in these two measurements are 1000 and 1900 Oe, respectively. The P_{MSBVW} power cited are calculated from the measured input microwave power and the one-way insertion loss of the respective MSW delay lines. In determination of actual input microwave drive power to the MO Bragg cell, the reflected power measured with a directional coupler was subtracted from the total input microwave power. The total insertion loss, which is the sum of the two-way conversion loss and the propagation loss of the MSW in the waveguide, was measured by a network analyzer. The propagation loss was estimated from the commonly used formula given by $76.4\Delta H\tau$[12] in which ΔH designates the FMR line width of the sample and τ the delay time. Using ΔH=0.3 Oe for the pure YIG sample and 1.3 Oe for the Bi-YIG sample, the one-way losses of the transducers were found to be -3.94 and -10dB, respectively. Finally, the linear dynamic ranges at the peak efficiency were measured to be 31 and 39 dB for, respectively, the pure YIG-GGG and the Bi-YIG-GGG Bragg cells. The dynamic range for the latter is presented in Fig.4.

Scanning of light beam in a waveguide structure has been a subject of continuing interest as it facilitates a variety of applications such as integrated-optic space switches and rf spectrum analyzers. One of the most actively explored techniques for this purpose utilizes Bragg diffraction of the light beam by the grating induced in the waveguide by surface acoustic waves (SAW) [13]. For example, integrated acoustooptic (AO) deflectors and rf spectrum analysers have been realized in $LiNbO_3$ [14] and GaAs [15] waveguide structures. A 4x4 integrated AO space switch has also been realized most recently [16]. In

the meantime, our earlier studies [8] have shown that in comparison to the SAWs magnetostatic waves (MSW) can operate at electronically-tunable rf carrier frequencies as high as 20 GHz and propagate at a velocity higher than the SAW by one to two-order of magnitude, and, thus provide higher switching speeds for the resulting devices by the same order of magnitude.

In our previous studies using the MSFVW-based MO Bragg cells, light beam scanning over the frequency ranges of 2.0-7.0 GHz and 3.7-12.0 GHz were accomplished by tuning the H_0 from 2000 to 3500 Oe and from 1430 to 4050 Oe for the pure-YIG- [4] and the Bi-YIG-GGG [5] waveguide samples, respectively. Using the same samples for our present study with the MSBVW, light beam scanning was accomplished in the same frequency range from the UHF-band (f<2.0 GHz) to the X-band (f>10 GHz) using ranges of significantly lower magnetic fields, namely, from 400 to 2800 Oe for the pure YIG-GGG and from 700 to 3400 Oe for the Bi-YIG-GGG waveguide samples. Light beam scanning could be accomplished at an even higher frequency if appropriate equipment were available in our laboratory. Figure 5(a) shows the photograph of a portion of the scanned light spots taken from the IR camera by tuning the carrier frequency starting at 7.83 GHz with H_0 fixed at 1913 Oe in the pure YIG-GGG sample. Figure 5(b) shows the photograph of the scanned light spots obtained by tuning the H_0 around 1949 Oe with a fixed carrier frequency of 7.80 GHz. Based on Figures 5(a) and 5(b), the frequency and DC magnetic field increments required for one fully-resolved beam spot varies, respectively, from 10 to 30 MHz and from 5 to 12 Oe. The measured frequency increment is smaller than that obtained with the MSFVW-based Bragg cells [4], namely, 18 to 36 MHz. By tuning the H_0 from 400 to 3400 Oe, light beam scanning from the UHF-band (f<2.0 GHz) to the X-band (f>10 GHz) can be performed with the same MO Bragg cell. For the Bi-YIG-GGG sample, the light beam scanning from 4.0 to 6.08 GHz was obtained with the H_0 fixed at 1927 Oe. Portion of the scanned light spots are shown in the photograph of Figure 5(c). The maximum Bragg diffraction angle for the Bi-doped

MSBVW-based Bragg cell was measured to be 12 degrees as compared to the maximum angle of 6 degrees previously measured with the MSFVW-based Bragg cells [3].

In conclusion, we have realized, for the first time, MSBVW-based MO Bragg cells in both pure YIG-GGG and Bi-doped YIG-GGG waveguides and accomplished wide-angle light beam scanning from the UHF-band (f<2.0 GHz) to the X-band (f>10 GHz). The measured performances of the MSBVW-based MO Bragg cells including the center frequency and its tuning range and the corresponding tuning range of DC magnetic field, location of the first passband, diffraction efficiency, microwave drive power, and the light beam scan angle were found to be superior to that of the MSFVW-based MO Bragg cells. Thus, we have established through theoretical and experimental studies the following advantages of the MSBVW over the MSFVW in terms of the performances of the resulting MO Bragg cells: (1) The center frequency of the MSBVW is higher than that of the MSFVW by some 4.9 GHz at the same DC magnetic field, (2) The first passband in which the MO Bragg cells commonly operate is located at the high frequency end for the MSBVW, but at the low frequency end for the MSFVW, and (3) The Bragg diffraction or mode-conversion efficiency of the MSBVW-based MO Bragg cells can be significantly higher than that of the MSFVW-based counterparts.

References

[1] (a) C.S. Tsai, "Hybrid integrated optic modules for real-time signal processing," Proc. of NASA Optical Information Processing Conference, NASA Conference Publication No. 2302, pp. 149-164 (1983).

(b) C.S. Tsai, D. Young, W. Chen, L. Adkins, C.C. Lee, and H. Glass, "Noncollinear coplanar magneto-optic interaction of guided optical wave and magnetostatic surface waves in yttrium iron garnet-gadolinium garnet waveguides," *Appl. Phys. Lett.*, 47, 651 (1985).

[2] See, for example, P.K. Tien and R.J. Martin, "Optical waveguides of crystal garnet films," *Appl. Phys. Lett.*, 21, 207 (1972); P.K. Tein, R.J. Martin, R. Wolfe, R.C.

LeCraw, and S.L. Blank, "Switching and modulation of light in magneto-optic waveguides of garnet films," *Appl. Phys. Lett.*, **21**, 394 (1972).

[3] D. Young and C.S. Tsai, "GHz bandwidth magnetooptic interaction in YIG-GGG waveguide using magnetostatic forward volume waves," *Appl. Phys. Lett.*, **53**, 1696 (1988).

[4] C.S. Tsai and D. Young, "Wideband scanning of guided-light beam and RF spectral analysis using magnetostatic forward volume waves in YIG-GGG waveguide," *Appl. Phys. Lett.*, **54**, 196 (1989).

[5] D. Young and C.S. Tsai, "X-band magnetooptic Bragg cells using bismuth-doped yttrium iron garnet waveguides," *Appl. Phys. Lett.*, **53**, 2242 (1989).

[6] K. Ando, N. Takeda, T. Okuda, and N. Koshizuka, "Waveguide mode conversion by magnetic linear birefringence of Bi-substituted iron garnet films tilted from (111)," *J. Appl. Phys.*, **57**, 718 (1985).

[7] H. Tamada, M. Kaneko, and T. Okamoto, "TM-TE optical-mode conversion induced by a transversely propagating magnetostatic wave in a (BiLu)3Fe5012 film," *J. Appl. Phys.*, **64**, 554 (1988).

[8] See, for example, the many references cited in the following paper, C.S. Tsai and D. Young, "Magnetostatic-forward-volume-wave-based guided-wave magneto-optic Bragg cells and applications to communications and signal processing," *IEEE Trans. on Microwave Theory and Techniques*, **38**, 560 (1990).

[9] A. Yariv, "Coupled-mode theory for guided-wave optics," *IEEE J. Quantum Electron.*, **QE-9**, 919 (1973).

[10] W.S. Ishak and K.W. Chang, "Magnetostatic-waves devices for microwave signal processing," *Hewlett-Packard Journal*, **36**, 10 (1985).

[11] Y. Pu and C.S. Tsai, "Magnetization of magnetostatic forward volume wave in YIG-GGG layered structure with application to guided-wave magnetooptic Bragg diffraction," *Proc. of 1990 Ultrasonic Symposium*, Dec. 5-7, Honolulu, Hawaii.

[12] J.D. Adam, "Delay of magnetostatic surface wave in YIG," *Electron. Lett.*, **6**, 718 (1970).

[13] See, for example, C.S. Tsai, "Guided-wave acoustooptic Bragg modulators for wideband integrated optic communications and signal processing," *IEEE Trans. Circuits Syst.*, **CAS-26**, 1072 (1972).

[14] See, for example, the many references cited in **Guided-Wave Acousto-optics**, edited by C.S. Tsai, Springer Series in Electronics and Photonics, Vol. 23 (1990).

[15] Y. Abdelrazek, C.S. Tsai, and T.Q. Vu, "An Integrated Optic RF Spectrum Analyzer in a ZnO-GaAs-AlGaAs Waveguide," *J. Lightwave Tech.*, **8**, 1833 (1990).

[16] C.S. Tsai and P. Le, "A 4x4 Nonblocking Integrated Acoustooptic Space Switch," (Accepted for publication in *Appl. Phys. Lett.*).

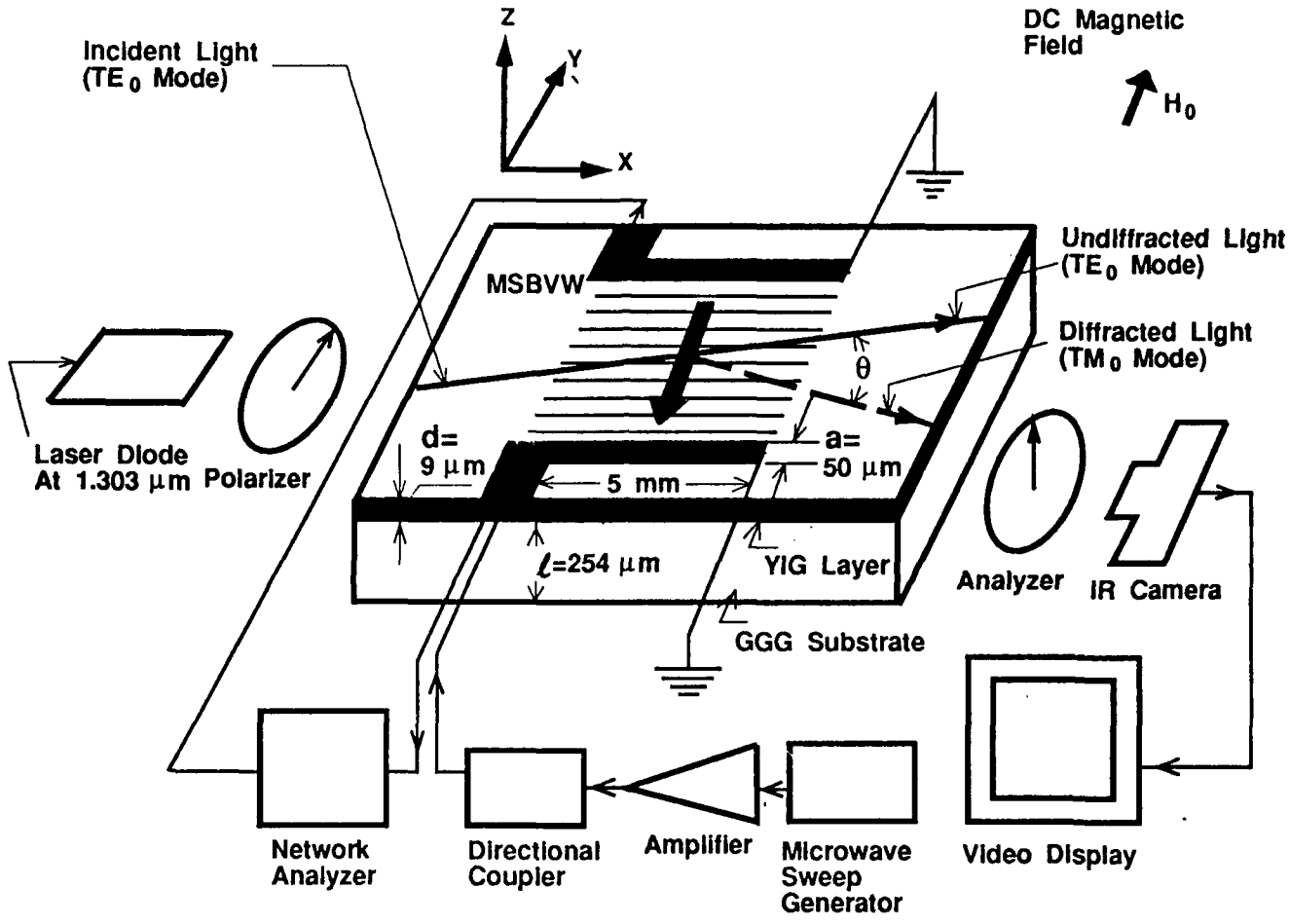

Fig.1 Geometry and Dimension of Magnetostatic Backward Volume Wave-Based Guided-Wave Magnetooptic Bragg Cells and Experimental Arrangement

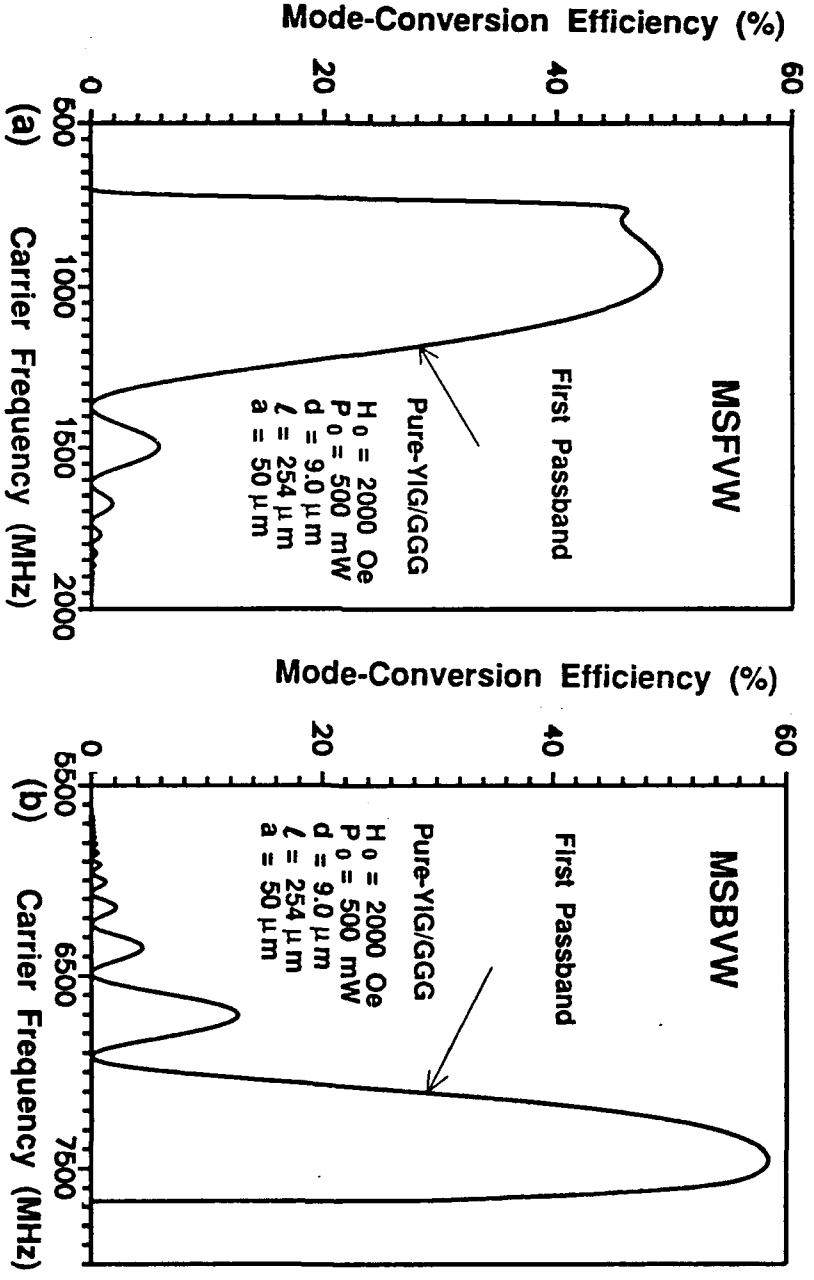

Fig.2 Guided-Wave Magnetooptic Mode-Conversion Efficiency Vs Carrier Frequency Using (a) MSFVW (b) MSBVW

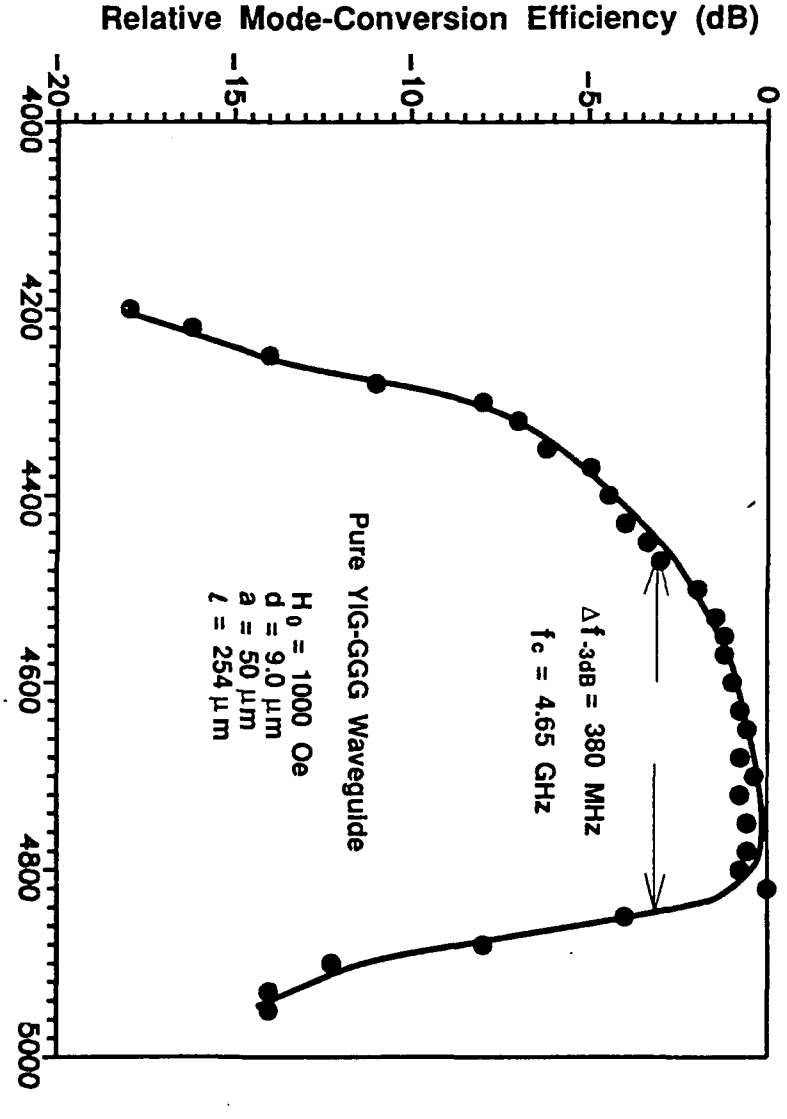

Fig.3(a) Measured First Passband of the Frequency Response of MSBVW-Based MO Bragg Cell in Pure YIG-GGG Waveguide

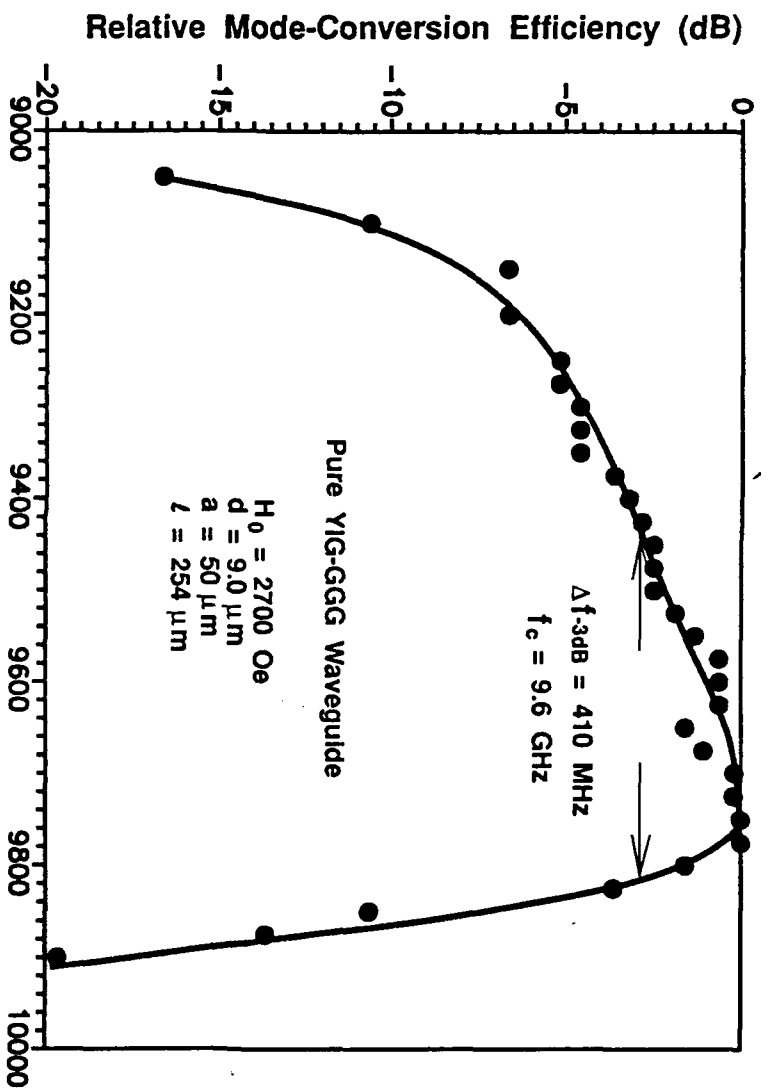

Fig.3(b) Measured First Passband of the Frequency Response of MSBVW-Based MO Bragg Cell in Pure YIG-GGG Waveguide

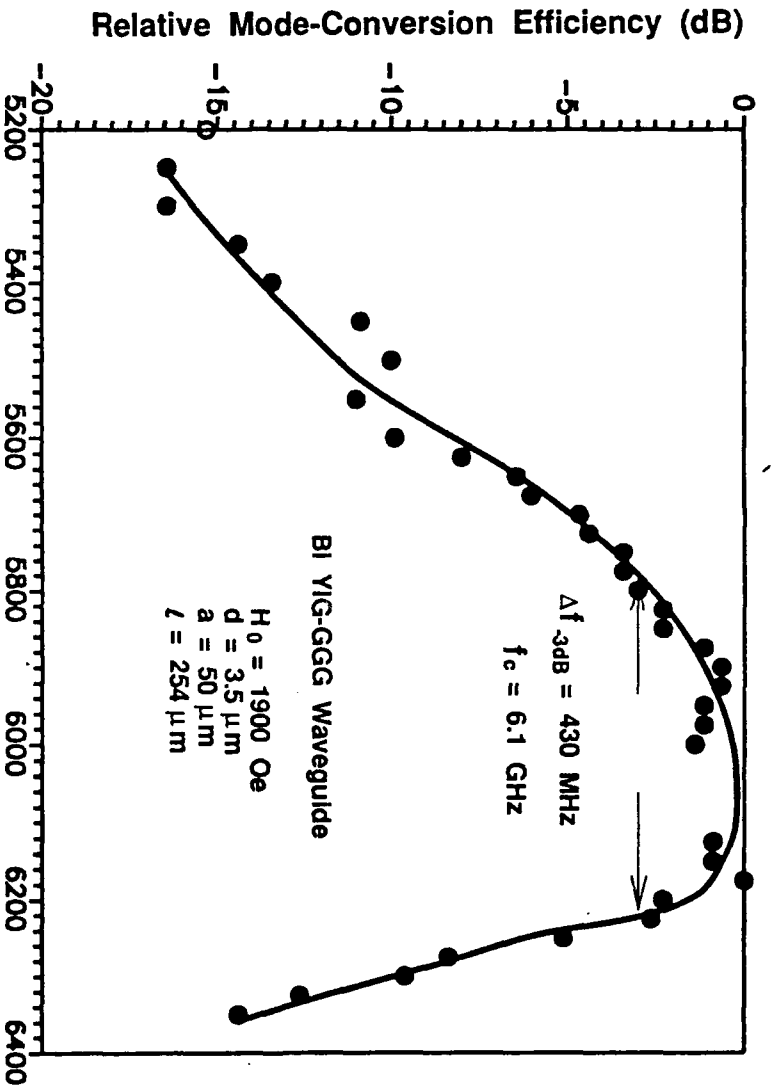

Fig.3(c) Measured First Passband of the Frequency Response of MSBVW-Based MO Bragg Cell in Bismuth-Doped YIG-GGG Waveguide

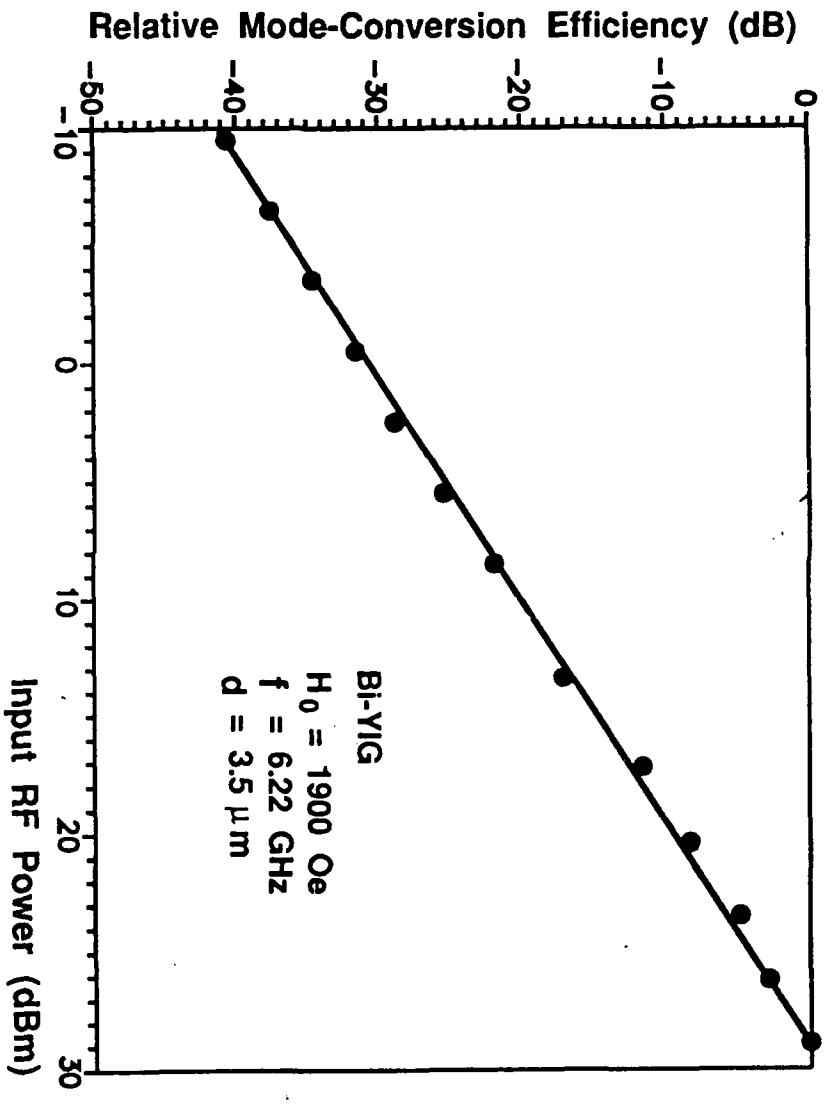

Fig.4 Magneto-optic Mode-Conversion (Diffraction) Efficiency Vs Microwave Drive Power for Bismuth-Doped YIG-GGG Guided-Wave Bragg Cell at the Carrier Frequency of 6.22 GHz

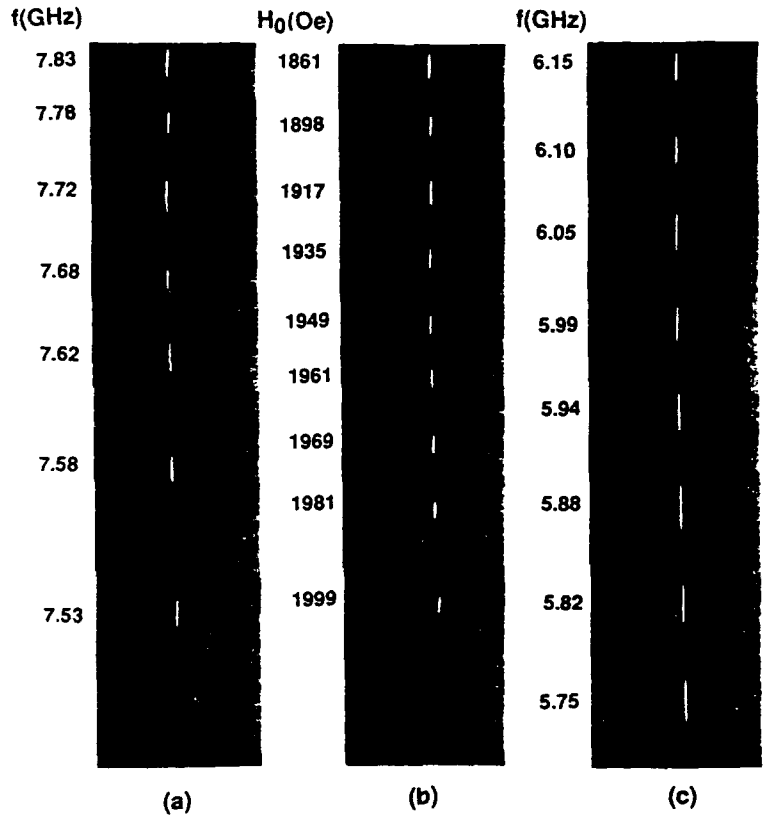

Fig.5 Scanned (Deflected) Light Beam Spots: (a) Vs Carrier Frequency at Fixed DC Magnetic Field of 1913 from Pure YIG MSBVW Bragg Cell; (b) Vs DC Magnetic Field at Fixed Carrier Frequency of 7.8 GHz from Pure YIG MSBVW Bragg Cell; (c) Vs Carrier Frequency at Fixed DC Magnetic Field of 1927 Oe from Bi-Doped YIG MSBVW Bragg Cell.

III. PUBLICATIONS RESULTING FROM ONR SUPPORT

1. Y. Pu and C.S. Tsai, "Magnetization of Magnetostatic Forward Volume Wave in a YIG-GGG Layered Structure with Application to Guided-Wave Magnetooptical Bragg Cell," Proc. of 1990 Ultrasonics Symposium, pp. 213-216, IEEE Cat. #: 90CH2938-9, ISSN: 1051-0117.

2. Y. Pu, C.L. Wang, and C.S. Tsai, "High-Performance Magnetostatic Backward Volume Waves-Based Guided Wave Magnetooptic Bragg Cells with Application to Wide-Angle Light Beam Scanning," Integrated Photonics Research, 1991. Technical Digest Series (Optical Society of America, Washington, D.C. 1991), pp. 20-21.

3. C.L. Wang, Y. Pu, and C.S. Tsai, "Compact Magnetostatic Wave-Based Magnetooptic Bragg Cell Module by Utilizing Small Permanent Magnet," Topical Meeting on Gradient-Index Optical Systems, 1991, Technical Digest Series (Optical Society of America, Washington, D.C.. 1991), pp. 74-77.

IV. TECHNICAL PERSONNEL

Principal Investigator:

Dr. Chen S. Tsai

Ph.D. Research Assistants:

1. C.L. Wang
2. Y. Pu
3. D. Grolemond

V. TECHNICAL INTERACTIONS

1. Dr. Matt White of ONR visited the group on March 21, 1991. A meaningful technical exchange was held among Dr. White, the research assistants and the principal investigator during his observation of actual magnetooptic Bragg diffraction and scanning experiment.

2. Dr. Tom Giallorenzi of the NRL visited the group on July 11, 1990 and observed the MO Bragg diffraction and scanning experiment.

3. Dr. A. N. Slavin of Shipbuilding Institute of Leningrad, USSR and Dr. Dan Stancil of Carnegie-Mellon University, both active in guided-wave magnetooptics research, visited the group and observed the MO experiment on November 2, 1990. A useful technical exchange was carried out during their visit.

4. Dr. Bob Adler from Zenith Electronics Co., a world-renown scientist and engineer in Bulk-Wave Acoustooptics, visited the group on November 6-9, 1990 and provided valuable suggestions in connection with the magnetic circuits that facilitate miniaturization of the MO Bragg cell.

5. Dr. Y. Okamura of Osaka University, Japan visited the group and observed the MO Bragg diffraction and scanning experiment on November 5, 1990.

6. Drs. Ali Ibrahim and Russel Raugh of Xerox Corp., El Segundo, California visited the group and observed the MO Bragg scanning experiment on November 6, 1990. A discussion was held in connection with potential application of the MO Bragg cells for high-speed light beam scanning and switching.